

Critical phase in a class of 1D quasiperiodic models with exact phase diagram and generalized dualities

Miguel Gonçalves,¹ Bruno Amorim,² Eduardo V. Castro,^{3, 4} and Pedro Ribeiro^{1, 4}

¹*CeFEMA, LaPMET, Instituto Superior Técnico,
Universidade de Lisboa, Av. Rovisco Pais, 1049-001 Lisboa, Portugal*

²*Centro de Física das Universidades do Minho e Porto, LaPMET,
University of Minho, Campus of Gualtar, 4710-057, Braga, Portugal*

³*Centro de Física das Universidades do Minho e Porto, LaPMET,
Departamento de Física e Astronomia, Faculdade de Ciências,
Universidade do Porto, 4169-007 Porto, Portugal*

⁴*Beijing Computational Science Research Center, Beijing 100193, China*

We propose a class of 1D quasiperiodic tight binding models that includes extended, localized and critical phases and analytically determine its phase diagram. Limiting cases of this class include the Aubry-André model and the models of Refs. [Phys. Rev. Lett. 114, 146601](#) and [Phys. Rev. Lett. 104, 070601](#). Away from these limits, critical multifractal phases are found to extend over a tunable region of parameters. Such critical phases are of practical interest as they host non-trivial mobility edges without the need of implementing unbounded potentials required by previous proposals. This class of models illustrates the most general duality symmetry found so far. It extends previously encountered duality transformations, between extended and localized phases, to dual points within the critical phase. The crucial observation of this work is to recognize these models as a novel class of fixed-points of the renormalization group procedure proposed in <http://arxiv.org/abs/2206.13549>. This allows to calculate the renormalized coefficients exactly and obtain a full analytical characterization of the phases of the infinite quasiperiodic system.

Quasiperiodic systems (QPS) offer a rich playground of interesting physics ranging from exotic localization properties in one [1–6] or higher [7–14] dimensions, to intriguing topological properties [15–19]. Quasiperiodicity arises in widely different platforms, including optical [2, 4, 5, 20–26] and photonic lattices [3, 12, 15, 17, 27, 28], cavity-polariton devices [29], phononic media [30–35] and moiré materials [36]. The ubiquity of QPS and their relevance to several interdisciplinary topical issues has rendered these systems a hot topic of research.

QPS host phases with fully localized and extended wave-functions. Interestingly, quasiperiodicity can also stabilize critical multifractal states, first encountered at the localization-delocalization transition lines, and later found to persist over extended regions [37–39], including in the presence of superconducting pairing [40–43].

However, QPS present substantial challenge for theoretical methods, and a fully analytical treatment of the localization phase diagrams remains restricted to a few fine-tuned models [1, 37, 44–49], and even a smaller subset hosts critical phases [37, 39]. In particular, Ref. [37], found critical phases with energy independent transitions to localized and delocalized phases, i.e. without mobility edges. These critical phases were shown to be robust to interactions, giving rise to a many-body critical regimes [50] and have been simulated using ultracold atoms [51]. A more generic scenario, where anomalous mobility edges found between critical and localized phases, was reported in Ref. [39] which, however, requires the use of unbounded quasiperiodic potentials. In

Ref. [52], the possibility of co-existence of extended, critical and localized regimes, separated by mobility edges, was numerically reported. As the existence of “anomalous” critical-to-extended or critical-to-localized mobility edges has not been experimentally reported so far, more models with no need for diverging potentials, are of topical and practical interest for experimental implementations.

Here, we propose a class of 1D quasiperiodic tight binding models that includes extended, localized and critical phases and analytically determine its phase diagram in the thermodynamic limit with a renormalization group procedure introduced in Ref. [53]. We show that these models represent a new class of fixed-points that contains as limiting cases the Aubry-André model and the models in Refs. [45, 48] with extended and localized phases. Away from these limits the model also contains critical phases that extend over a considerable region of parameters, as shown in Fig. 1(a).

We show that duality transformations previously found in Refs. [45, 48] between localized and delocalized states are limiting cases of a more general duality that extends to non-self-dual states within the critical phase, as shown in Fig. 1. For the proposed model, such duality transformation is not locally confined to the vicinity of self-dual lines. Instead, it is valid globally across the phase diagram.

In what follows, we present the model, obtain the analytical expressions for the phase boundaries of all its phases, including mobility edges between extended and

localized phases, and anomalous critical-to-extended and critical-to-localized mobility edges. Finally, we discuss the implications of our findings.

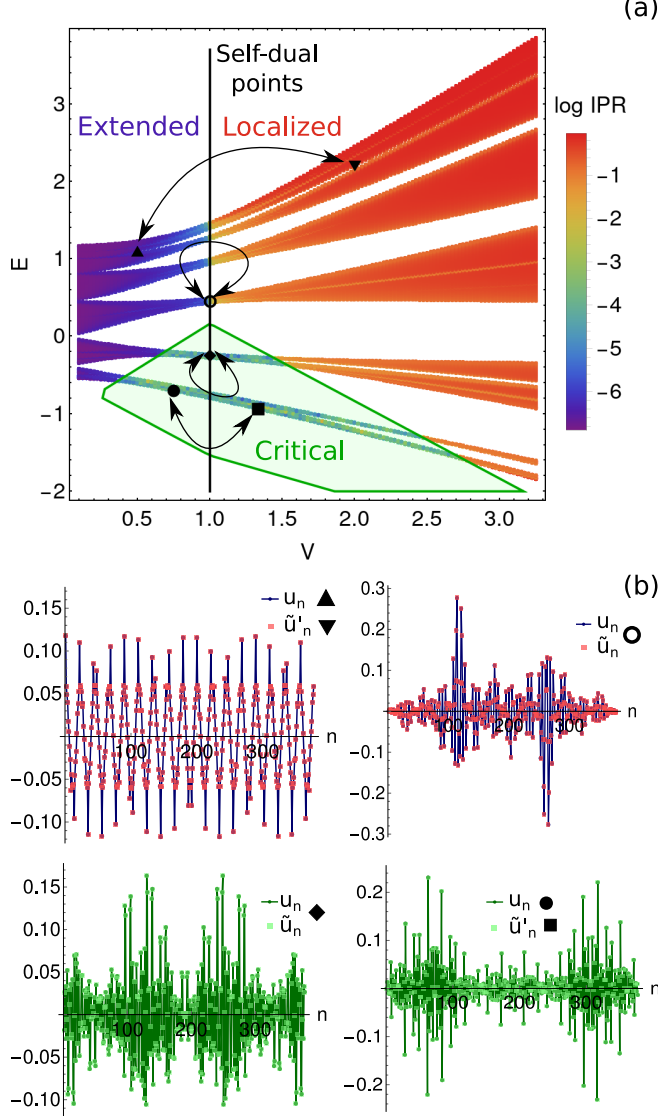


FIG. 1. (a) IPR (see Eq. (4) for definition) results obtained numerically for $L = F_{16} = 987$ and $p = q = 1$. The analytical phase boundaries between the extended and localized phases (self-dual points) and of the critical phase (green lines) are superimposed with the numerical results. (b) Examples of eigenstates u_n and dual eigenstates \tilde{u}'_n defined in Eq. (6) at dual points in the phase diagram indicated in (a). For these states we used $L = F_{14} = 377$. Notice that since $p = q$, $W(x) = 1$ and \tilde{u}'_n and u_n are simply related by the Aubry-André duality.

Model and methods.— We consider a family of models parameterized by the Hamiltonian

$$H = t \sum_{n \neq n'} e^{i\alpha(n-n')} e^{-p|n-n'|} c_n^\dagger c_{n'} + 2V \sum_n \sum_{l=1}^{+\infty} e^{-ql} \cos[l(2\pi\tau n + \phi)] c_n^\dagger c_n \quad (1)$$

where c_n^\dagger creates a particle at site n . The first term describes hopping elements modulated by a magnetic flux α with an exponential decay determined by p . The second term represents a quasiperiodic potential, incommensurate with the lattice for $\tau \neq \mathbb{Q}$, obtained by summing harmonics of the incommensurate wavenumber $2\pi\tau$ with exponentially decaying amplitudes controlled by the parameter l . In the following we set $t = 1$ unless otherwise stated.

The model in Eq. (1) reduces to that in [45] in the $q \rightarrow \infty$ limit and $\alpha = 0$ after the replacing $t \rightarrow te^p$ and $V \rightarrow Ve^q$. Similarly, it reduces to the model in [48] for large p , and to the Aubry-André model when both p and q are large.

We consider finite systems with L sites. In order to avoid boundary defects when applying twisted boundary conditions, the numerical results were obtained by considering rational approximants of the irrational parameter τ . We chose τ to be the inverse of the golden ratio in the numerical calculations, but our analytical results for the phase diagram are independent of τ . The rational approximants can be written as $\tau_c^{(n)} = F_{n-1}/F_n$, where F_n is a Fibonacci number that defines the number of sites in the unit cell for the choice $\tau_c^{(n)}$. For this choice, the system size is taken to be $L = F_n$ [54, 55]. Imposing twisted boundary conditions, with phase twists k , is the same as working in a fixed momentum sector of the Hamiltonian in the Bloch basis,

$$c_n \rightarrow c_{m,r} = \frac{1}{\sqrt{N}} \sum_k e^{ik(m+rL)} \tilde{c}_{m,k}, \quad (2)$$

where $m = 0, \dots, L-1$ runs over the sites of the unit cell of size L , and $r = 0, \dots, N$ is the unit cell index, with $N \rightarrow \infty$ the total number of unit cells. The Hamiltonian for a fixed k -sector then becomes

$$H(k) = t \sum_{r=-\infty}^{\infty} \sum_{m,m'=0}^{L-1} e^{-p|rL+m-m'|} e^{i(\alpha-k)(m+rL-m')} \tilde{c}_{m,k}^\dagger \tilde{c}_{m',k} + 2V \sum_{m=0}^{L-1} \sum_{l=1}^{+\infty} e^{-ql} \cos[l(2\pi\tau_c m + \phi)] \tilde{c}_{m,k}^\dagger \tilde{c}_{m,k} \quad (3)$$

which is just the Hamiltonian of a system with L sites and a phase twist k .

To analytically characterize the phase diagram for this family of models we use the methods introduced by us

in Ref. [53] and an exact generalized duality that we prove below. Our analytical results are confirmed numerically through the real-space and momentum-space inverse participation ratios, respectively IPR and IPR_k . For an eigenstate $|\psi(E)\rangle = \sum_n \psi_n(E) |n\rangle$, where $\{|n\rangle\}$ is a basis localized at each site, these quantities are defined as [56]

$$\text{IPR}_{(k)}(E) = \frac{\sum_n |\psi_n^{(k)}(E)|^4}{(\sum_n |\psi_n^{(k)}(E)|^2)^2}, \quad (4)$$

where $\psi_n^k(E)$ are the amplitudes of the discrete Fourier transform of the set $\{\psi_n(E)\}$. In the extended (localized) phase, the $\text{IPR}(\text{IPR}_k)$ scales as L^{-1} , with L the total number of sites, while in the localized (extended) phase it is L -independent for large enough L . At a critical point or critical phase, the wave function is multifractal: it is delocalized in real and momentum-space and both the IPR and IPR_k scale down with L [56].

Exact duality.— The Schrödinger equation for the model in Eq. (3) with phase twists k can be written as

$$h_n u_n - \sum_{m=-\infty}^{\infty} e^{i(\alpha-k)(n-m)} e^{-p|n-m|} u_m = 0, \quad (5)$$

where $h_n = \eta - V\chi(q, 2\pi\tau n + \phi)$, $\eta = E + t + V$ and $\chi(\lambda, x) = \sum_l e^{-\lambda|l|} e^{ilx} = \sinh \lambda [\cosh \lambda - \cos(x)]^{-1}$. At dual points $P(t, V, p, q, \alpha, E; \phi, k)$ and $P'(t', V', p', q', \alpha', E'; \phi', k')$, this equation can be mapped into a dual equation under the duality transformation (see SM for proof)

$$\tilde{u}_n = \sum_m e^{i2\pi\tau nm} W(2\pi\tau m) u_m, \quad (6)$$

where $W(x) = \chi(q', x + \phi') \chi^{-1}(p, x + k - \alpha)$. The dual points P and P' satisfy

$$\begin{cases} \phi' = k - \alpha + \pi \frac{(s-1)}{2}, \quad -k' + \alpha' = \phi + \pi \frac{(s-1)}{2} \\ \frac{D(V', \eta', p', q')}{B(V', \eta', p')} = s \frac{D(V, \eta, p, q)}{A(V, \eta, q)} \\ \frac{A(V', \eta', q')}{B(V', \eta', p')} = \frac{B(V, \eta, p)}{A(V, \eta, q)} \\ \frac{\eta'}{B(V', \eta', p')} = s \frac{\eta}{A(V, \eta, q)} \end{cases} \quad (7)$$

where $s = \pm 1$ and

$$\begin{aligned} A(V, \eta, q) &= -\eta \cosh q + V \sinh q \\ B(V, \eta, p) &= -\eta \cosh p + t \sinh p \\ D(V, \eta, p, q) &= \eta \cosh p \cosh q - t \cosh q \sinh p \\ &\quad - V \cosh p \sinh q. \end{aligned} \quad (8)$$

For fixed $p = q$, Eq. (6) defines the usual Aubry-André duality.

The self-duality condition is imposed by choosing $P = P'$. In this case, Eq. (7) is solved simply through the condition $A(V, \eta, q) = \pm B(V, \eta, p)$, that yields the following equation for the self-dual points:

$$E = \frac{V \sinh q \mp t \sinh p}{\cosh q \mp \cosh p} - t - V. \quad (9)$$

The global duality transformation defined in Eq. (6) was confirmed to match the definition given in Ref. [57] in terms of commensurate approximants (CA). CA are defined by the rational ratio $\tau_c = L'/L$, where L' and L are two co-prime integers and L is the number of sites in the CA's unit cell. The definition introduced in Ref. [57] allows, for a given CA, to calculate L samples of the duality function $W'(x) \propto W(2\pi x)$ at points $x_n = L'n/L, n = 0, \dots, L-1$ (see SM). Examples of the dual transformation are given in Fig. 2 and demonstrate that the global duality defined by Eq. 6 matches the numerical results.

Besides the global dualities shown here, that occur for points satisfying Eqs. 7, local dualities also arise close to the SD points even along directions in the parameter space where the global duality in Eq. (7) breaks down [57]. In Fig. 2 we show an example of globally dual points connected by the global duality in Eq. (6) and locally dual points, computed numerically through CA as detailed in [57]. We also show examples for duality functions $W'(x)$ obtained at locally dual points (according to the previous definition) in Fig. 2(b) [58].

Phase diagram.— We are finally in position to analytically obtain the complete phase diagram. The transitions between extended and localized phases obtained through the IPR/IPR_k calculations perfectly match the SD points described by Eq. (9). Examples are shown in Fig. 1(a) for $p = q$, when Eq. (9) reduces to the Aubry-André energy independent self-dual line $V = t$, and Fig. 3(a,b) for $p \neq q$. However, the SD points can also occur within the critical phase, in which case they are not associated with any transition. This implies that the phase boundaries of the critical phase are not described by SD points, as noticed in Ref. [53] for other models.

To obtain the full phase diagram analytically we make use of the renormalization-group approach developed in Ref. [53]. In fact, the model studied here is a fixed-point model according to the classification in [53] albeit of a novel universality class. Its characteristic polynomial for a CA with L sites (see SM) is

$$\begin{aligned} \mathcal{P}_L(\varphi, \kappa) &= V_L \cos(\varphi) + t_L \cos(\kappa) \\ &\quad + C_L \cos(\varphi) \cos(\kappa) + D_L, \end{aligned} \quad (10)$$

where $\varphi = L\phi$, $\kappa = Lk$ and V_L, t_L, C_L and D_L are renormalized couplings. For the simplest CA (one site

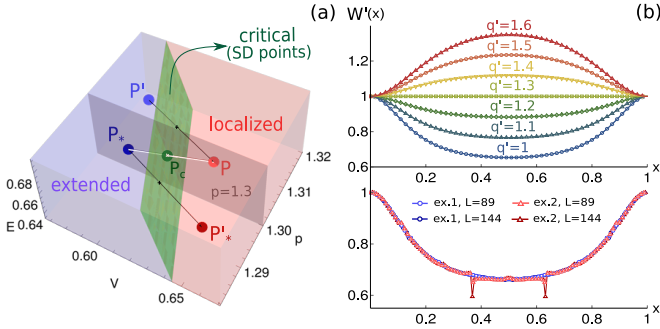


FIG. 2. (a) Example of globally dual points obeying the global duality in Eq. (6) (sets of points $P \leftrightarrow P'$ and $P_* \leftrightarrow P'_*$ connected by black lines), locally dual points obeying local hidden dualities ($P \leftrightarrow P_*$ connected by white line) and a self-dual critical point P_c . P, P_* and P_c belong to the plane $p = 1.3$ where the global duality does not hold except at SD points such as P_c , which in this example separate extended and localized phases. For this figure, we have set $q = q' = 1$ (b) Top: Duality function $W'(x) \propto W(2\pi x)$ for a point P defined by $p = 1.3, q = 1, V \approx 0.73, E \approx 0.34$, and different dual points parameterized by different values of q' (the remaining dual parameters, V', p' and E' were obtained by solving Eq. (7) for the different choices of q'). Note that even though P is fixed, the duality transformation depends on P' (in particular on q'), in accordance with the definition in Eq. (6). The data points correspond to the $L = 55$ samples of the duality function $W'(x)$ obtained for a CA with $\tau_c = 34/55$ (see SM for details). The full lines are plots of the exact analytical duality function in Eq. (6). The latter was normalized so that $W(0) = W'(0)$. Bottom: Examples of samples of $W'(x)$ for different dual points within the plane $p = 1.3$, for $\tau_c = 55/89$ and $\tau_c = 89/144$ (the points for the different CA were chosen to be the closest possible to each other).

per unit cell), we have, using the definitions in Eq. (8), that $t_1 = A(V, \eta, q)$, $V_1 = B(V, \eta, p)$, $C_1 = \eta$ and $D_1 = D(V, \eta, p, q)$. The ratios between the renormalized couplings V_L, t_L and C_L can be computed exactly. If $|t_1/C_1| > 1$ or $|V_1/C_1| > 1$, we have, respectively

$$|t_L/C_L| = |g_L^+(t_1/C_1) + g_L^-(t_1/C_1)|/2 \quad (11)$$

$$|V_L/C_L| = |g_L^+(V_1/C_1) + g_L^-(V_1/C_1)|/2 \quad (12)$$

where $g_L^\pm(x) = (x \pm \sqrt{x^2 - 1})^L$. On the other hand, if $|C_1/t_1| > 1$ or $|C_1/V_1| > 1$ we have, respectively

$$|t_L/C_L| = |T_L(t_1/C_1)| \quad (13)$$

$$|V_L/C_L| = |T_L(V_1/C_1)| \quad (14)$$

where $T_L(x)$ is the L -th order Chebyshev polynomial. It is easy to see that if $|t_1/V_1|, |t_1/C_1| > 1$ we have that

$|t_L/V_L|, |t_L/C_L| \rightarrow \infty$ exponentially in L as $L \rightarrow \infty$, i.e. we are in the extended phase. For $|V_1/t_1|, |V_1/C_1| > 1$, we have $|V_L/t_L|, |V_L/C_L| \rightarrow \infty$ and the phase is localized. Finally, $|C_1/t_1|, |C_1/V_1| > 1$ ensures that $|C_L/t_L|, |C_L/V_L| > 1$ for any L (a property of Chebyshev polynomials), and the system is in a critical phase. Therefore, the phases and phase boundaries are fully determined through the previous conditions by knowing the functions in Eq. (8). Summarizing, phases and phase boundaries are analytically given by

$$\begin{aligned} |A/B|, |A/\eta| &> 1, \text{Ext.} \\ |B/A|, |B/\eta| &> 1, \text{Loc.} \\ |\eta/A|, |\eta/B| &> 1, \text{Crit.} \end{aligned} \quad (15)$$

$$\begin{aligned} |A| = |B|, |A|, |B| &> |\eta|, \text{Ext.-to-Loc.} \\ |A| = |\eta|, |A|, |\eta| &> |B|, \text{Crit.-to-Ext.} \\ |B| = |\eta|, |B|, |\eta| &> |A|, \text{Crit.-to-Loc.} \end{aligned} \quad (16)$$

where we omitted the parameter dependence for clarity. From the ratios of renormalized couplings we are also able to calculate the correlation lengths in the extended and localized phases in terms of A, B and η (see SM). Note that the renormalized couplings only depend on the size of the unit cell and not on the specific approximant. This implies that the $L \rightarrow \infty$ limit defines the phase diagram for any τ .

To confirm our analytical results, we show in Figs. 3(b-d) some examples of finite-size scaling results that agree with the analytical phase boundaries here unveiled. Note that while in the extended-to-localized transitions both the IPR and IPR_k scale down only at the critical point [Fig. 3(b)], such scaling is observed for the entire range of the critical phase when the latter exists [Fig. 3(c-d)].

Discussion.— We have analytically obtained the phase diagram for a class of models that are shown to host critical multifractal phases in addition to localized and delocalized ones. To our knowledge, this represents the largest and richest family of one-dimensional quasiperiodic exactly solvable models, from which previously known instances [1, 45, 48] can be obtained as limiting cases. We show that these models obey a global generalized duality symmetry. The key observation to derive our results is to recognize that this class of models corresponds to a novel set of fixed-points of the Renormalization-Group (RG) procedure developed in Ref. [53]. These findings show that the RG treatment can be extended to critical phases, in which case the duality transformation maps phase-space points within the critical phase. These results demonstrate a non-trivial instance where the RG method can be used to solve models with analytically-tractable phase diagrams.

From a practical perspective, the family of models we propose is attractive to implement in flexible setups

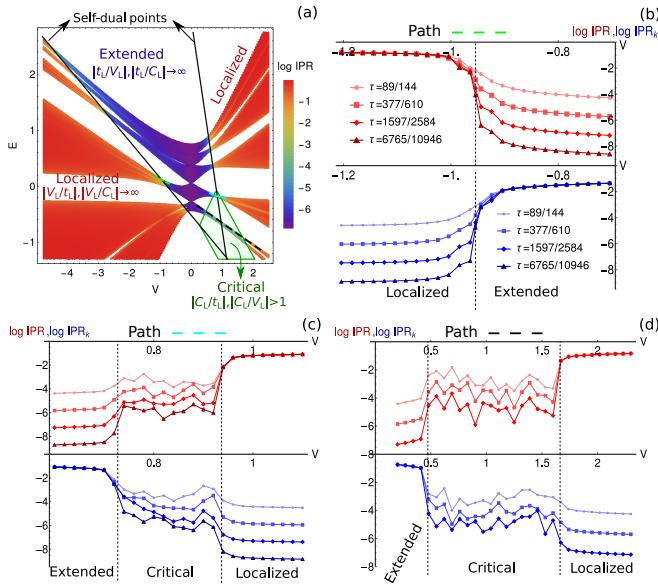


FIG. 3. (a) IPR results obtained for $p = 1.3, q = 1$ and $L = F_{16} = 987$, superimposed with the analytical curves for SD points (black) and phase boundaries of the critical phase (green). In each phase, we also show the asymptotic results of the renormalized couplings as $L \rightarrow \infty$. (b-d) Finite-size scalings of the IPR (red) and IPR_k (blue) for points (V, E) across the paths shown in the dashed curves in (a). The results were averaged over 70, 25, 16 and 6 random shifts ϕ and twists k , respectively for increasing $L \in [144, 10946]$. The dashed vertical lines correspond to the analytical results for the phase boundaries.

where exponentially decaying hoppings and quasiperiodic harmonics can be engineered, such as optical, photonic, or phononic lattices. In particular, they allow realizing a critical phase with mobility edges without the need for unbounded potentials, as previously proposed in Ref. [39]. This renders the model a well-suited test-bed to study the robustness to interactions of mobility edges and critical phases.

The authors MG and PR acknowledge partial support from Fundação para a Ciência e Tecnologia (FCT-Portugal) through Grant No. UID/CTM/04540/2019. BA and EVC acknowledge partial support from FCT-Portugal through Grant No. UIDB/04650/2020. MG acknowledges further support from FCT-Portugal through the Grant SFRH/BD/145152/2019. BA acknowledges further support from FCT-Portugal through Grant No. CEECIND/02936/2017. We finally acknowledge the Tianhe-2JK cluster at the Beijing Computational Science Research Center (CSRC) and the OBLIVION supercomputer (based at the High Performance Computing Center - University of Évora) funded by the ENGAGE SKA Research Infrastructure (reference POCI-01-0145-FEDER-022217 - COMPETE 2020 and the Foundation for Science and Technology, Portugal) and by the Big-Data@UE project (reference ALT20-03-0246-FEDER-

000033 - FEDER) and the Alentejo 2020 Regional Operational Program. Computer assistance was provided by CSRC and the OBLIVION support team.

- [1] S. Aubry and G. André, *Proceedings, VIII International Colloquium on Group-Theoretical Methods in Physics* **3** (1980).
- [2] G. Roati, C. D'Errico, L. Fallani, M. Fattori, C. Fort, M. Zaccanti, G. Modugno, M. Modugno, and M. Inguscio, *Nature* **453**, 895 (2008), [arXiv:0804.2609](https://arxiv.org/abs/0804.2609).
- [3] Y. Lahini, R. Pugatch, F. Pozzi, M. Sorel, R. Morandotti, N. Davidson, and Y. Silberberg, *Physical Review Letters* (2009), [10.1103/PhysRevLett.103.013901](https://doi.org/10.1103/PhysRevLett.103.013901).
- [4] M. Schreiber, S. S. Hodgman, P. Bordia, H. P. Lüschen, M. H. Fischer, R. Vosk, E. Altman, U. Schneider, and I. Bloch, *Science* **349**, 842 (2015), [arXiv:1501.05661](https://arxiv.org/abs/1501.05661).
- [5] H. P. Lüschen, S. Scherg, T. Kohlert, M. Schreiber, P. Bordia, X. Li, S. Das Sarma, and I. Bloch, *Physical Review Letters* (2018), [10.1103/PhysRevLett.120.160404](https://doi.org/10.1103/PhysRevLett.120.160404).
- [6] D. S. Borgnia, A. Vishwanath, and R.-J. Slager, “*Rational approximations of quasi-periodic problems via projected green's functions*,” (2021).
- [7] C. Huang, F. Ye, X. Chen, Y. V. Kartashov, V. V. Konotop, and L. Torner, *Scientific Reports* **6**, 32546 (2016).
- [8] J. H. Pixley, J. H. Wilson, D. A. Huse, and S. Gopalakrishnan, *Phys. Rev. Lett.* **120**, 207604 (2018).
- [9] M. J. Park, H. S. Kim, and S. Lee, *Phys. Rev. B* **99**, 245401 (2019), [arXiv:1812.09170](https://arxiv.org/abs/1812.09170).
- [10] B. Huang and W. V. Liu, *Phys. Rev. B* **100**, 144202 (2019).
- [11] Y. Fu, E. J. König, J. H. Wilson, Y.-Z. Chou, and J. H. Pixley, *npj Quantum Materials* **5**, 71 (2020).
- [12] P. Wang, Y. Zheng, X. Chen, C. Huang, Y. V. Kartashov, L. Torner, V. V. Konotop, and F. Ye, *Nature* (2020), [10.1038/s41586-019-1851-6](https://doi.org/10.1038/s41586-019-1851-6), [arXiv:2009.08131](https://arxiv.org/abs/2009.08131).
- [13] M. Gonçalves, H. Z. Olyaei, B. Amorim, R. Mondaini, P. Ribeiro, and E. V. Castro, “*Incommensurability-induced sub-ballistic narrow-band-states in twisted bilayer graphene*,” (2020), [arXiv:2008.07542 \[cond-mat.mes-hall\]](https://arxiv.org/abs/2008.07542).
- [14] P. Bordia, H. Lüschen, S. Scherg, S. Gopalakrishnan, M. Knap, U. Schneider, and I. Bloch, *Phys. Rev. X* **7**, 041047 (2017).
- [15] Y. E. Kraus, Y. Lahini, Z. Ringel, M. Verbin, and O. Zilberberg, *Physical Review Letters* (2012), [10.1103/PhysRevLett.109.106402](https://doi.org/10.1103/PhysRevLett.109.106402), [arXiv:1109.5983](https://arxiv.org/abs/1109.5983).
- [16] Y. E. Kraus and O. Zilberberg, *Phys. Rev. Lett.* **109**, 116404 (2012).
- [17] M. Verbin, O. Zilberberg, Y. E. Kraus, Y. Lahini, and Y. Silberberg, *Physical Review Letters* (2013), [10.1103/PhysRevLett.110.076403](https://doi.org/10.1103/PhysRevLett.110.076403), [arXiv:1211.4476](https://arxiv.org/abs/1211.4476).
- [18] O. Zilberberg, *Opt. Mater. Express* **11**, 1143 (2021).
- [19] D. S. Borgnia and R.-J. Slager, “*Localization via quasi-periodic bulk-bulk correspondence*,” (2021).
- [20] D. J. Boers, B. Goedeke, D. Hinrichs, and M. Holthaus, *Phys. Rev. A* **75**, 63404 (2007).
- [21] M. Modugno, *New Journal of Physics* **11**, 33023 (2009).
- [22] H. Yao, H. Khoudli, L. Bresque, and L. Sanchez-Palencia, *Phys. Rev. Lett.* **123**, 070405 (2019).

[23] H. Yao, T. Giamarchi, and L. Sanchez-Palencia, *Phys. Rev. Lett.* **125**, 060401 (2020).

[24] R. Gautier, H. Yao, and L. Sanchez-Palencia, *Phys. Rev. Lett.* **126**, 110401 (2021).

[25] F. A. An, K. Padavić, E. J. Meier, S. Hegde, S. Ganeshan, J. H. Pixley, S. Vishveshwara, and B. Gadway, *Phys. Rev. Lett.* **126**, 040603 (2021).

[26] T. Kohlert, S. Scherg, X. Li, H. P. Lüschen, S. Das Sarma, I. Bloch, and M. Aidelsburger, *Phys. Rev. Lett.* **122**, 170403 (2019).

[27] M. Verbin, O. Zilberberg, Y. Lahini, Y. E. Kraus, and Y. Silberberg, *Phys. Rev. B* **91**, 64201 (2015).

[28] A. D. Sinelnik, I. I. Shishkin, X. Yu, K. B. Samusev, P. A. Belov, M. F. Limonov, P. Ginzburg, and M. V. Rybin, *Advanced Optical Materials* **8**, 2001170 (2020), <https://onlinelibrary.wiley.com/doi/pdf/10.1002/adom.202001170>.

[29] V. Goblot, A. Štrkalj, N. Pernet, J. L. Lado, C. Dorow, A. Lemaître, L. Le Gratiet, A. Harouri, I. Sagnes, S. Ravets, A. Amo, J. Bloch, and O. Zilberberg, *Nature Physics* (2020), 10.1038/s41567-020-0908-7.

[30] D. J. Apigo, W. Cheng, K. F. Dobiszewski, E. Prodan, and C. Prodan, *Phys. Rev. Lett.* **122**, 095501 (2019).

[31] X. Ni, K. Chen, M. Weiner, D. J. Apigo, C. Prodan, A. Alù, E. Prodan, and A. B. Khanikaev, *Communications Physics* **2**, 55 (2019).

[32] W. Cheng, E. Prodan, and C. Prodan, *Phys. Rev. Lett.* **125**, 224301 (2020).

[33] Y. Xia, A. Erturk, and M. Ruzzene, *Phys. Rev. Applied* **13**, 014023 (2020).

[34] Z.-G. Chen, W. Zhu, Y. Tan, L. Wang, and G. Ma, *Phys. Rev. X* **11**, 011016 (2021).

[35] M. Gei, Z. Chen, F. Bosi, and L. Morini, *Applied Physics Letters* **116**, 241903 (2020), <https://doi.org/10.1063/5.0013528>.

[36] L. Balents, C. R. Dean, D. K. Efetov, and A. F. Young, *Nat. Phys.* **16**, 725 (2020).

[37] F. Liu, S. Ghosh, and Y. D. Chong, *Phys. Rev. B - Condens. Matter Mater. Phys.* **91**, 014108 (2015).

[38] X. Deng, S. Ray, S. Sinha, G. V. Shlyapnikov, and L. Santos, *Phys. Rev. Lett.* **123**, 025301 (2019).

[39] T. Liu, X. Xia, S. Longhi, and L. Sanchez-Palencia, *SciPost Phys.* **12**, 27 (2022).

[40] W. DeGottardi, D. Sen, and S. Vishveshwara, *Phys. Rev. Lett.* **110**, 146404 (2013).

[41] J. Wang, X.-J. Liu, G. Xianlong, and H. Hu, *Phys. Rev. B* **93**, 104504 (2016).

[42] T. Čadež, R. Mondaini, and P. D. Sacramento, *Physical Review B* (2019), 10.1103/PhysRevB.99.014301, [arXiv:1808.10238](https://arxiv.org/abs/1808.10238).

[43] Y. Wang, L. Zhang, S. Niu, D. Yu, and X.-J. Liu, *Phys. Rev. Lett.* **125**, 073204 (2020).

[44] M. Johansson and R. Riklund, *Phys. Rev. B* **43**, 13468 (1991).

[45] J. Biddle and S. Das Sarma, *Phys. Rev. Lett.* **104**, 70601 (2010).

[46] J. D. Bodyfelt, D. Leykam, C. Danieli, X. Yu, and S. Flach, *Phys. Rev. Lett.* **113**, 236403 (2014).

[47] C. Danieli, J. D. Bodyfelt, and S. Flach, *Phys. Rev. B* **91**, 235134 (2015).

[48] S. Ganeshan, J. H. Pixley, and S. Das Sarma, *Phys. Rev. Lett.* **114**, 146601 (2015).

[49] T. Liu, X. Xia, S. Longhi, and L. Sanchez-Palencia, arXiv e-prints , arXiv:2105.04591 (2021), [arXiv:2105.04591 \[cond-mat.dis-nn\]](https://arxiv.org/abs/2105.04591).

[50] Y. Wang, C. Cheng, X.-J. Liu, and D. Yu, *Phys. Rev. Lett.* **126**, 080602 (2021).

[51] T. Xiao, D. Xie, Z. Dong, T. Chen, W. Yi, and B. Yan, *Science Bulletin* **66**, 2175 (2021).

[52] Y. Wang, L. Zhang, W. Sun, and X.-J. Liu, “Quantum phase with coexisting localized, extended, and critical zones,” (2022).

[53] M. Gonçalves, B. Amorim, E. V. Castro, and P. Ribeiro, (2022), 10.48550/arxiv.2206.13549, [arXiv:2206.13549](https://arxiv.org/abs/2206.13549).

[54] M. Y. Azbel, *Phys. Rev. Lett.* **43**, 1954 (1979).

[55] M. Kohmoto, *Phys. Rev. Lett.* **51**, 1198 (1983).

[56] C. Aulbach, A. Wobst, G.-L. Ingold, P. HÄEnggi, and I. Varga, *New Journal of Physics* **6**, 70 (2004).

[57] M. Gonçalves, B. Amorim, E. V. Castro, and P. Ribeiro, arXiv e-prints , arXiv:2103.03895 (2021), [arXiv:2103.03895 \[cond-mat.dis-nn\]](https://arxiv.org/abs/2103.03895).

[58] The local duality function may be very sensitive to the choice of the correct dual points. Since their computation was done numerically, there is an associated error. Therefore we slightly varied the computed dual point and checked that some features may arise only due to a slightly incorrect choice of this point (see SM).

[59] We set $\phi = k = 0$ from here on.

[60] W. R. Inc., “Mathematica, Version 12.3.1,” Champaign, IL, 2021.

Supplemental Material for:

CONTENTS

Acknowledgments	5
References	5
S1. Derivation of generalized global duality transformation	SM - 1
S2. Details on the calculation of local dualities for commensurate approximants	SM - 3
S3. Derivation of ratios between renormalized couplings	SM - 4

S1. DERIVATION OF GENERALIZED GLOBAL DUALITY TRANSFORMATION

Our starting point is the Schrödinger equation

$$h_n u_n = \sum_m e^{i(\alpha-k)(n-m)} f(|n-m|) u_m, \quad (\text{S1})$$

where $h_n = \eta - V\chi_n(q, \phi)$, $\eta = E + t + V$, $f(|n-m|) = te^{-p|n-m|}$ and $\chi_m(q, \phi) = \frac{\sinh q}{\cosh q - \cos(2\pi\tau m + \phi)}$. k is a phase twist while α was chosen to be a parameter of the model. From here on we will absorb the parameter α in the twist k , that is $k - \alpha \rightarrow k$. In what follows we will also use the useful identity

$$\chi_m(q, \phi) = \frac{\sinh q}{\cosh q - \cos(2\pi\tau m + \phi)} = \sum_{l=-\infty}^{+\infty} e^{-q|l|} e^{i(2\pi\tau m + \phi)l}. \quad (\text{S2})$$

In [57] we have seen that generic duality transformations for Aubry-André-like systems may be defined as

$$\tilde{u}_n = \sum_m e^{i2\pi\tau nm} W_m u_m. \quad (\text{S3})$$

Here we will find the form of W_m for which an exact global duality of the type in Eq. (S3) can be defined. The inverse transformation is

$$u_m = \frac{1}{N} W_m^{-1} \sum_n e^{-i2\pi\tau nm} \tilde{u}_n, \quad (\text{S4})$$

where N is the total number of sites in the system. Writing Eq. (S1) in terms of the dual wave function \tilde{u}_n , we have

$$h_n W_n^{-1} \sum_m e^{-i2\pi\tau nm} \tilde{u}_m = \sum_m e^{-ik(n-m)} f(|n-m|) W_m^{-1} \sum_l e^{-i2\pi\tau ml} \tilde{u}_l. \quad (\text{S5})$$

Multiplying by $e^{i2\pi\tau n\mu}$ and summing over n , we get

$$\sum_m \left[\sum_n e^{i2\pi\tau n(\mu-m)} W_n^{-1} (h_n - \chi_\mu(p, -k)) \right] \tilde{u}_m = 0. \quad (\text{S6})$$

Our aim now is to find W_n such that Eq. (S6) for some point $P(t, V, p, q, \alpha, E; \phi, k)$, is dual of Eq. (S1) at a dual point $P'(t', V', p', q', \alpha', E'; \phi', k')$. For convenience, we write Eq. (S1) as

$$\Lambda_\mu \left(\sum_m [h_m \delta_{m,\mu} - e^{-ik(\mu-m)} e^{-p|\mu-m|}] u_m \right) = 0. \quad (\text{S7})$$

Notice that Λ_μ is an additional degree of freedom that does not affect the solution of Eq. (S1): we want to inspect when equations (S1) and (S6) are equal under a suitable choice of Λ_μ . Imposing an equality for these equations term by term, we have

$$\Lambda_\mu \left(h_m \delta_{m,\mu} - e^{-ik(\mu-m)} e^{-p|\mu-m|} \right) = \sum_n e^{i2\pi\tau n(\mu-m)} W_n^{-1} \left(h'_n - \chi_\mu(p', -k') \right). \quad (\text{S8})$$

From Eq. (S8), we obtain

$$W_l = \gamma_\mu \frac{h'_l - \chi_\mu(p', -k')}{h_\mu - \chi_l(p, k)} = \gamma_\mu \frac{\eta' - V' \chi_l(q', \phi') - \chi_\mu(p', -k')}{\eta - V \chi_\mu(q, \phi) - \chi_l(p, k)} \equiv \gamma_\mu P_{\mu l}, \quad (\text{S9})$$

where $\gamma_\mu = \Lambda_\mu^{-1}$. Note that the right-hand-side is a tensor. This means that W_l is only well defined, that is, a duality transformation of the type in Eq. (S3) only exists, if we can write $P_{\mu l} = p_\mu W_l$, so that γ_μ can be chosen as p_μ^{-1} . This cannot be done in general. Defining $c_{\mu,k} = \cos(2\pi\tau\mu + k)$ and $c_{\mu,\phi} = \cos(2\pi\tau\mu + \phi)$, we have

$$W_l = \gamma_\mu \left(\frac{c_{\mu,\phi} - \cosh q}{c_{\mu,-k'} - \cosh p'} \right) \left(\frac{c_{l,k} - \cosh p}{c_{l,\phi'} - \cosh q'} \right) \frac{B(V', \eta', p')}{A(V, \eta, q)} \left(\frac{\frac{D(V', \eta', p', q')}{B(V', \eta', p')} + \frac{A(V', \eta', q')}{B(V', \eta', p')} c_{\mu,-k'} + c_{l,\phi'} + \frac{\eta'}{B(V', \eta', p')} c_{\mu,-k'} c_{l,\phi'}}{\frac{D(V, \eta, p, q)}{A(V, \eta, q)} + \frac{B(V, \eta, p)}{A(V, \eta, q)} c_{\mu,\phi} + c_{l,k} + \frac{\eta}{A(V, \eta, q)} c_{\mu,\phi} c_{l,k}} \right) \quad (\text{S10})$$

where, as in the main text, we have

$$\begin{aligned} A(V, \eta, q) &= -\eta \cosh q + V \sinh q \\ B(V, \eta, p) &= -\eta \cosh p + \sinh p \\ D(V, \eta, p, q) &= \eta \cosh p \cosh q - \cosh q \sinh p - V \cosh p \sinh q \end{aligned} \quad (\text{S11})$$

The last term in Eq. (S10) is the only problematic term, for which the indexes μ and l do not decouple. However, if we require the numerator and denominator to be equal, this term will be equal to 1 and W_l becomes well-defined for any choice of γ_μ that cancels the μ -dependence. This is, for instance, the case if (note the change of phases ϕ and k):

$$\begin{cases} k' = -\phi; \phi' = k \\ \frac{D(V', \eta', p', q')}{B(V', \eta', p')} = \frac{D(V, \eta, p, q)}{A(V, \eta, q)} \\ \frac{A(V', \eta', q')}{B(V', \eta', p')} = \frac{B(V, \eta, p)}{A(V, \eta, q)} \\ \frac{\eta'}{B(V', \eta', p')} = \frac{\eta}{A(V, \eta, q)} \end{cases} \quad (\text{S12})$$

The choice

$$\begin{cases} k' = -\phi + \pi; \phi' = k + \pi \\ \frac{D(V', \eta', p', q')}{B(V', \eta', p')} = -\frac{D(V, \eta, p, q)}{A(V, \eta, q)} \\ \frac{A(V', \eta', q')}{B(V', \eta', p')} = \frac{B(V, \eta, p)}{A(V, \eta, q)} \\ \frac{\eta'}{B(V', \eta', p')} = -\frac{\eta}{A(V, \eta, q)} \end{cases} \quad (\text{S13})$$

is equally valid. The first choice implies that $A(V, \eta, q) = B(V, \eta, p)$ at self-dual points, while the second implies that $A(V, \eta, q) = -B(V, \eta, p)$. Alternatively, we could choose $k' = -\phi + \pi$ and $\phi' = k$ or $k' = -\phi$ and $\phi' = k + \pi$. But

these choices give rise to contradicting equations at the self-dual points. The equations for dual points written in Eqs. (S12) and (S13) are summarized in the main text.

Finally, if we choose

$$\gamma_\mu = \frac{A(V, \eta, q) \sinh q (c_{\mu, -k'} - \cosh p')}{B(V', \eta', p') \sinh p (c_{\mu, \phi} - \cosh q)}, \quad (\text{S14})$$

we get, from Eq. (S10), that

$$W_l = \chi_l(q', \phi') \chi_l^{-1}(p, k). \quad (\text{S15})$$

We finally check some limiting cases that were already known in the literature. The first case is the Aubry-André model which is recovered from our model if we make the substitutions $t \rightarrow te^p$ and $V \rightarrow Ve^q/2$ and then take the large p limit, with $p = q = p' = q'$. Nonetheless, even if we do not take the large p limit, just by setting these latter equalities we get $W_l = 1$, implying that $\tilde{u}_n = \sum_m e^{i2\pi\tau nm} u_m$, which is just the original Aubry-André duality transformation [1]. The dual points can also be obtained from Eqs. (S12), (S13) to be $V' = 4t^2/V$ and $E' = \pm 2Et/V$, as obtained in Ref. [1] (the \pm signs come respectively from Eqs. (S12), (S13)).

We can also check the large q limit that corresponds to the limit in [45] if we make $t \rightarrow te^p$ and $V \rightarrow Ve^q$. In this case, $\chi_l(q', \phi') \rightarrow 1$ and we obtain the duality transformation in this reference. On the other hand, in the large p limit we get the model in Ref. [48] making again the previous substitutions. In this limit, $\chi_l^{-1}(p, k) \rightarrow 1$ and we get the dual transformation proven in Ref. [57] at self-dual points. Even though the duality transformations were used only to find self-dual points in Refs. [45, 48], they can also be used to define other dual points that can be found through Eqs. S12, S13.

We finally remark that away from the previously mentioned limits, the duality transformation depends both on the starting and dual points. Even though this was a possibility introduced in [57], the transformation in Eq. (S15) was, as far as the authors are aware, the first found global exact duality of this type.

S2. DETAILS ON THE CALCULATION OF LOCAL DUALITIES FOR COMMENSURATE APPROXIMANTS

To compute the data points used in Fig. 2(b), corresponding to samples of the duality function $W'(x)$, we followed the procedure introduced in [57]. Given dual points P and P' in the parameter space [59] for a given CA defined by $\tau_c = L'/L$ (L, L' co-prime integers), we define $u^r(P')$ as the solution to Eq. (5) at point P' and $u^d(P)$ as

$$u_n^d(P) = \frac{1}{\sqrt{L}} \sum_{m=0}^{L-1} e^{i2\pi\tau_c mn} u_n^r(P). \quad (\text{S16})$$

As in Ref. [57], we define the duality matrix \mathcal{O}_c in terms of $u^r(P')$ and $u^d(P)$ as

$$\mathcal{O}_c[T^n u^d(P)] = T^n u^r(P'), \quad n = 0, \dots, L-1, \quad (\text{S17})$$

where T is the cyclic translation operator defined as $T\psi = \psi'$ with $\psi'_i = \psi \bmod (i+1, L)$. Since \mathcal{O}_c is a circulant matrix, we may write it as

$$\mathcal{O}_c = U^\dagger W' U \quad (\text{S18})$$

where U is a matrix with entries $U_{\mu\nu} = e^{2\pi i \frac{L'}{L} \mu\nu}$ and W' is a diagonal matrix $W'_{\mu\nu} = w'_\mu \delta_{\mu\nu}$ with the eigenvalues w'_μ of \mathcal{O}_c . We can therefore write

$$u^r(P') = U^\dagger W' u^r(P) \leftrightarrow u_\mu^r(P') = \sum_{\nu=0}^{L-1} e^{2\pi i \tau_c \mu\nu} w'_\nu u_\nu^r(P). \quad (\text{S19})$$

The eigenvalues w'_ν are, as seen in Ref. [57], evaluations of a function $W'(x)$, that has period $\Delta x = 1$, at points $x_\nu = \mod(\nu\tau_c, 1)$, $\nu = 0, \dots, L-1$. This function is continuously sampled in the limit that $\tau_c \rightarrow \tau$, that is, as $L \rightarrow \infty$. At global dual points defined by Eqs. 7 of the main text, the exact duality transformation is defined in Eq. (6) that we rewrite below:

$$\tilde{u}_\mu(P') = \sum_\nu e^{i2\pi\tau\mu\nu} W(\tau\nu) u_\nu(P) \quad (\text{S20})$$

where $W(x) = \chi(q', x)\chi^{-1}(p, x)$ and $\chi(\lambda, x) = \sinh \lambda [\cosh \lambda - \cos(2\pi x)]^{-1}$. In the commensurate limit, replacing $\tau \rightarrow \tau_c$ in Eq. (S20), we find that

$$w'_\nu = W'(\tau_c\nu) \propto W(\tau_c\nu). \quad (\text{S21})$$

The duality function $W(x)$ can therefore be sampled at L different points by computing the eigenvalues w'_ν for CA with L sites in the unit cell. They were computed and shown as data points in Fig. 2(b) of the main text together with the exact analytical duality function to confirm the validity of the latter.

In the case of local dualities, the exact duality function is unknown and the only way to access it is by computing the eigenvalues w'_ν at (locally) dual points. In this case, dual points were computed numerically as explained in Ref. [57]. As shown in one of the examples in Fig. 2(b) of the main text, the duality function for the local dualities can be highly non-trivial.

We finish by remarking that it is important to precisely compute the dual points to get a meaningful duality function. While for the global dualities the dual points can be calculated exactly, this is not the case for the local dualities for which there are unavoidable numerical errors. In Fig. S1 we show an example where it can be seen that even a small numerical error in the calculation of dual points may introduce artificial features to the function $W'(x)$: we must therefore slightly change the dual point with respect to the computed one and check the robustness of function $W'(x)$. In this example we checked that the dual point was miscalculated with an error in the parameter V of $\Delta V \approx 0.0001$, that was corrected to present the results of Fig. 2(b) of the main text.

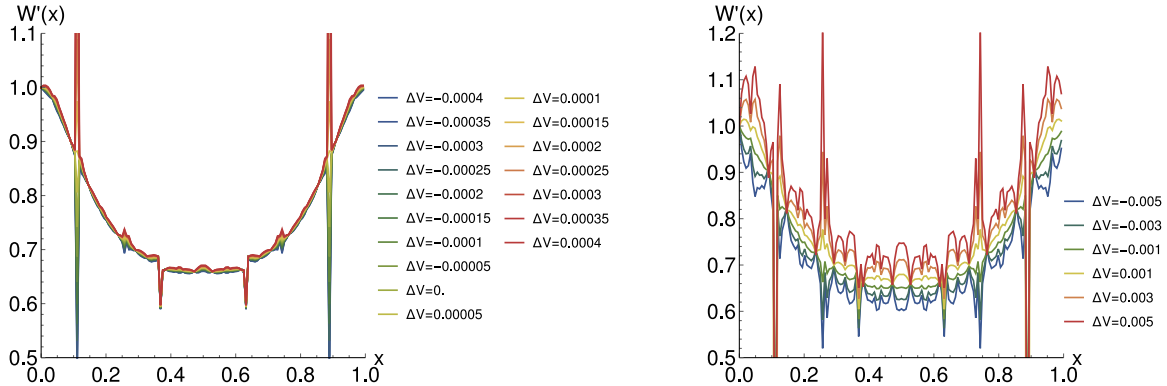


FIG. S1. $W'(x)$ obtained by linear interpolation of the eigenvalues w'_ν for $\tau_c = 89/144$, for the parameters defining the duality transformation in Fig. 2(b) (bottom, red) of the main text. We considered a starting point P with $p = 1.3, q = 1, V \approx 0.73015, E \approx 0.34580$ and points P' with $p' = 1.3, q' = 1, V' \approx 0.67439 + \Delta V, E' \approx 0.33609$. The point for $\Delta V = 0$ corresponds to the dual point computed numerically. In fact, the smoothest function is obtained for the point with $\Delta V \approx 0.0001$ for which the sharp features close to $x = 0.1$ and $x = 0.9$ are removed (left figure). This suggests that the latter is the true dual point and that even a small numerical error may lead to the appearance of artificial features. If we move away from the true dual point (right figure), the duality function becomes very noisy and meaningless.

S3. DERIVATION OF RATIOS BETWEEN RENORMALIZED COUPLINGS

Our starting point is Eq. (S1) for a commensurate system defined by $\tau = \tau_c = L'/L$, where L' and L two co-prime integers and L defines the number of sites in the unit cell. In this case, we have $h_{n+rL} = h_n$ and Bloch's theorem warrants $u_{n+rL} = u_n, n = 0, \dots, L-1, r \in \mathbb{Z}$.

We start by considering the example of one site per unit cell, that is, $\tau_c = 1$. In this case, the Schrödinger equation becomes

$$\left[h_0 - t \sum_m e^{ikm} f(|m|) \right] u_0 = 0,$$

which can be written as

$$[\eta - V\chi_0(q, \phi) - t\chi_0(p, k)] u_0 = 0,$$

with χ_0 given by Eq. (S2). Noticing that $[\cosh q - \cos(\phi)][\cosh p - \cos(k)] \neq 0$ we have

$$[A(V, \eta, q) \cos(k) + B(V, \eta, p) \cos(\phi) + \eta \cos(\phi) \cos(k) + D(V, \eta, p, q)] = 0. \quad (\text{S22})$$

Equation. (S22) defines the characteristic polynomial for the simplest CA. To characterize higher-order CA, we start by applying the transformation $\sum_{n=0}^{L-1} e^{i2\pi\tau_c n \mu} = \frac{L}{N} \sum_n e^{i2\pi\tau_c n \mu}$, where N is the total number of sites in the system. The first term in Eq. (S1) becomes

$$\sum_{n=0}^{L-1} e^{i2\pi\tau_c n \mu} h_n u_n = \frac{L}{N} \sum_m e^{i2\pi\tau_c m \mu} h_m u_m, \text{ with } h_{m+rL} = h_m, r \in \mathbb{Z}. \quad (\text{S23})$$

For the second term we have (absorbing again α in the phase twist k):

$$\frac{L}{N} \sum_n e^{i2\pi\tau_c n \mu} \sum_m e^{-ik(n-m)} f(|n-m|) u_m$$

Using $m' = n - m$: (S24)

$$\frac{L}{N} \sum_{m'} e^{i2\pi\tau_c \mu m'} e^{-ikm'} f(|m'|) \sum_m e^{i2\pi\tau_c m \mu} u_m = \frac{L}{N} \chi(p, 2\pi\tau_c \mu - k) \sum_m e^{i2\pi\tau_c m \mu} u_m,$$

where we used Eq. (S2) and defined $\chi(\lambda, x) \equiv \chi_0(\lambda, x)$. In the commensurate case, we only sample the function $\chi(\lambda, x)$ at a discrete set of points $x_\mu = 2\pi\tau_c \mu - k$, $\mu = 0, \dots, L-1$. Combining Eqs. (S23) and (S24), we get

$$\begin{aligned} & \sum_m e^{i2\pi\tau_c m \mu} [h_m - \chi(p, 2\pi\tau_c \mu - k)] u_m = 0 \\ \Leftrightarrow & \sum_m e^{i2\pi\tau_c m \mu} \left(\frac{A(V, \eta, q) c_{\mu, -k} + B(V, \eta, p) c_{m, \phi} + \eta c_{m, \phi} c_{\mu, -k} + D(V, \eta, p, q)}{[\cosh q - c_{m, \phi}][\cosh p - c_{\mu, -k}]} \right) u_m = 0 \\ \Leftrightarrow & M\mathbf{u} = 0 \end{aligned} \quad (\text{S25})$$

where we used the short-hand notation $c_{m, \phi} = \cos(2\pi\tau_c m + \phi)$ and $c_{\mu, k} = \cos(2\pi\tau_c \mu + k)$ and $\mathbf{u} = (u_0, \dots, u_{L-1})$. Note that each component $M_{\mu m}$ is now written in a form that resembles Eq. (S22) for the simplest CA. In particular, we essentially made appear the characteristic polynomial for this CA for every term, with the difference that now the phase ϕ is associated with index m and the phase $-k$ with index μ .

We will now compute the ϕ - and k -dependent parts of the determinant of matrix M in Eq. (S25). Our final aim is to calculate the ratios between renormalized couplings $|t_L/C_L|, |V_L/C_L|$ and $|t_L/V_L|$, where these couplings are defined, for the characteristic polynomial of a CA with L sites in the unit cell, $\mathcal{P}_L(\varphi, \kappa)$, as

$$\mathcal{P}_L(\varphi, \kappa) = V_L \cos(\varphi) + t_L \cos(\kappa) + C_L \cos(\varphi) \cos(\kappa) + \dots \quad (\text{S26})$$

where $\varphi = L\phi$ and $\kappa = Lk$. On the way, we will also explain why only the fundamental harmonics in φ and κ appear for any CA.

We start by noting that the denominator of each term $M_{\mu m}$ can be written as $T_{\mu\phi} T'_{mk} = [\cosh q - c_{\mu, \phi}][\cosh p - c_{m, -k}]$. The Leibniz formula for the determinant is

$$\det(M) = \sum_{\sigma \in S_L} \operatorname{sgn}(\sigma) \prod_{\mu=0}^{L-1} M_{\mu, \sigma_\mu} \quad (\text{S27})$$

where S_L is the set of permutations of indexes $i = 1, \dots, L$. Therefore for each term in the sum we get all the possible combinations of $T_{\mu\phi} T'_{\mu k}$, that is if we write $M_{\mu m} = P_{\mu m} / (T_{\mu\phi} T'_{\mu k})$, we have

$$\det(M) = \frac{1}{\prod_{\mu} T_{\mu\phi} T'_{\mu k}} \sum_{\sigma \in S_L} \operatorname{sgn}(\sigma) \prod_{\mu=0}^{L-1} P_{\mu, \sigma_\mu} \propto \sum_{\sigma \in S_L} \operatorname{sgn}(\sigma) \prod_{\mu=0}^{L-1} P_{\mu, \sigma_\mu}. \quad (\text{S28})$$

Let us focus on the $|t_L/C_L|$ ratio. We have

$$\det(M) \propto \sum_{\sigma \in S_L} \operatorname{sgn}(\sigma) \prod_{\mu=0}^{L-1} e^{i2\pi\tau_c \mu \sigma_\mu} \left(\eta c_{\mu, -k} \left(\frac{A}{\eta} + c_{\sigma_\mu, \phi} \right) + B c_{\sigma_\mu, \phi} + D \right). \quad (\text{S29})$$

We first realize that only products of terms $\eta c_{\mu, -k} (A/\eta + c_{\sigma_\mu, \phi})$ matter to get the terms $t_L \cos(\kappa) + C_L \cos(\kappa) \cos(\phi)$ of $\mathcal{P}_L(\varphi, \kappa)$. This is because to obtain terms with L times the original frequency k or ϕ (recall the definitions $\varphi = L\phi$ and $\kappa = Lk$), we need to have L products of terms $c_{\mu, -k}$ and $c_{\mu, \phi}$. The only way to accomplish this is by multiplying L terms of the type $\eta c_{\mu, -k} (A/\eta + c_{\sigma_\mu, \phi})$. At this point, we can also ask why terms of the type $\cos(nx)$ with $x = \phi, k$ and $n \in \mathbb{N} < L$ do not appear in $\mathcal{P}_L(\varphi, \kappa)$. This would give rise to periodicities in ϕ and k , $\Delta\phi, \Delta k > 2\pi/L$, that are forbidden. The twist k is nothing more than a Bloch momentum associated with the unit cell of size L : the reciprocal lattice vector for this unit cell is $G = 2\pi/L$ and therefore the energy bands should repeat with a period $\Delta k = 2\pi/L$. In the case of phase ϕ , shifts $\Delta\phi = 2\pi/L$ in a CA with a unit cell with L sites are just re-definitions of this unit cell [57]. The energy bands should therefore be periodic upon these shifts. Finally, we can also ask why we cannot have terms of the type $\cos(nx)$ with $x = \phi, k$ and $n \in \mathbb{N} > L$. The reason is that such terms would require a number of $n > L$ products of terms $c_{\mu, -k}$ and $c_{\mu, \phi}$ that do not appear in the determinant in Eq. S29. Therefore, we only have fundamental harmonics in φ and κ , as previously stated.

To make further progress, we will need the following identity for L, L' two co-prime integers [60],

$$\prod_{\mu=0}^{L-1} \left[\cos(y) - \cos \left(\frac{2\pi L' \mu}{L} + \phi \right) \right] = 2^{1-L} \left[\cos(Ly) - \cos(L\phi) \right], \quad (\text{S30})$$

which we can apply to the term $\sum_{\sigma \in S_L} \operatorname{sgn}(\sigma) \prod_{\mu=0}^{L-1} e^{i2\pi\tau_c \mu \sigma_\mu} \eta c_{\mu, -k} \left(\frac{A}{\eta} + c_{\sigma_\mu, \phi} \right)$ in Eq. (S29), as long as $|A/\eta| < 1$ (which occurs inside the critical phase) by identifying $y = \arccos A/\eta$. We then obtain

$$\begin{aligned} \det(M) &\propto \gamma_{\sigma} \left(-\cos(L\pi/2) + \cos(Lk) \right) \left(\cos[L \arccos(A/\eta)] - \cos(L\phi) \right) + \sum_{\sigma \in S_L} \operatorname{sgn}(\sigma) \prod_{\mu=0}^{L-1} e^{i2\pi\tau_c \mu \sigma_\mu} (B c_{\sigma_\mu, \phi} + D) \\ &\propto \cos[L \arccos(A/\eta)] \cos(Lk) - \cos(Lk) \cos(L\phi) + \dots \end{aligned} \quad (\text{S31})$$

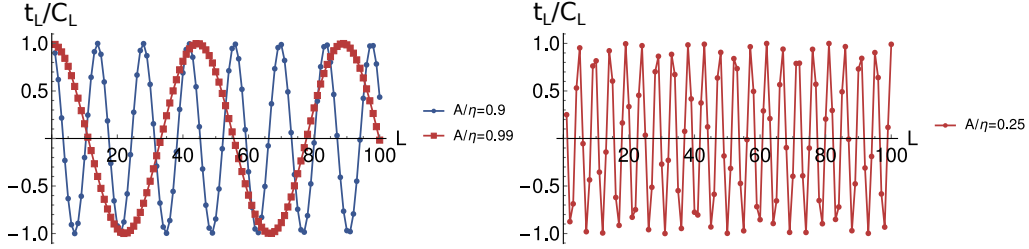
where we identified

$$\gamma_{\sigma} = \sum_{\sigma \in S_L} \operatorname{sgn}(\sigma) \prod_{\mu=0}^{L-1} e^{i2\pi\tau_c \mu \sigma_\mu}. \quad (\text{S32})$$

We therefore have that

$$|t_L/C_L| = |\cos[L \arccos(A/\eta)]| = |T_L(A/\eta)| \quad (\text{S33})$$

where $T_L(x)$ is the Chebyshev polynomial of order L . It is very interesting to realize that there is no well-defined limit of $|t_L/C_L|$ for large L . In fact, even though we always have $|t_L/C_L| < 1$, its value oscillates with L with a period that becomes larger the closer $|A/\eta|$ is to 1 (being infinity at $|A/\eta| = 1$). Examples are shown in Fig. S2.

FIG. S2. t_L/C_L for different $|A/\eta| < 1$.

What about $|A| \geq |\eta|$? In this case, it is useful to use the following property [60]:

$$\prod_{\mu=0}^{L-1} \left[x \pm y \cos \left(\frac{2\pi L' \mu}{L} + \phi \right) \right] = \frac{1}{2^L} \left[\left(x + \sqrt{x^2 - y^2} \right)^L + \left(x - \sqrt{x^2 - y^2} \right)^L - 2(\mp y)^L \cos(L\phi) \right]. \quad (\text{S34})$$

This may again be applied to the term $\sum_{\sigma \in S_L} \text{sgn}(\sigma) \prod_{\mu=0}^{L-1} e^{i2\pi\tau_c \mu \sigma_\mu} \eta c_{\mu,-k}(\frac{A}{\eta} + c_{\sigma_\mu, \phi})$ in Eq. (S29), by identifying $x = A/\eta$ and $y = 1$. In this case we obtain

$$|C_L/t_L| = \frac{2}{\left(\left| \frac{A}{\eta} \right| + \sqrt{\left(\frac{A}{\eta} \right)^2 - 1} \right)^L + \left(\left| \frac{A}{\eta} \right| - \sqrt{\left(\frac{A}{\eta} \right)^2 - 1} \right)^L}. \quad (\text{S35})$$

Note that with $|A/\eta| > 1$ this gives an exponential decay for $|C_L/t_L|$. This is just what we expect in the extended phase, where the dominant coupling is t_L , regarding that it also dominates over V_L . At large L we have $|C_L/t_L| \sim e^{-L/\xi_{\text{EC}}}$, and the decay length ξ_{EC} is

$$\xi_{\text{EC}} = \frac{1}{\log \left[|A/\eta| + \sqrt{(A/\eta)^2 - 1} \right]}, \quad (\text{S36})$$

which is finite for any $|A/\eta| > 1$ and of course diverges for $|A/\eta| = 1$ (transition between extended and critical phase).

With identical calculations, we can work out the expressions for $|C_L/V_L|$ just by replacing A with B everywhere above. This yields

$$|V_L/C_L| = \begin{cases} |T_L(B/\eta)| & , |B/\eta| < 1 \\ \frac{1}{2} \left[\left(\left| \frac{B}{\eta} \right| + \sqrt{\left(\frac{B}{\eta} \right)^2 - 1} \right)^L + \left(\left| \frac{B}{\eta} \right| - \sqrt{\left(\frac{B}{\eta} \right)^2 - 1} \right)^L \right] & , |B/\eta| \geq 1 \end{cases}. \quad (\text{S37})$$

For $|B/\eta| \geq 1$ we get the following correlation length characterizing the localized-critical transition:

$$\xi_{\text{LC}} = \frac{1}{\log \left[|B/\eta| + \sqrt{(B/\eta)^2 - 1} \right]}. \quad (\text{S38})$$

The ratio $|t_L/V_L|$ may then be obtained through the previous expressions. For $|V_L/C_L|, |t_L/C_L| > 1$ (outside the critical phase), we have

$$|t_L/V_L| = \frac{\left(\left| \frac{A}{\eta} \right| + \sqrt{\left(\frac{A}{\eta} \right)^2 - 1} \right)^L + \left(\left| \frac{A}{\eta} \right| - \sqrt{\left(\frac{A}{\eta} \right)^2 - 1} \right)^L}{\left(\left| \frac{B}{\eta} \right| + \sqrt{\left(\frac{B}{\eta} \right)^2 - 1} \right)^L + \left(\left| \frac{B}{\eta} \right| - \sqrt{\left(\frac{B}{\eta} \right)^2 - 1} \right)^L}. \quad (\text{S39})$$

We have seen in Ref. [53] that the correlation or localization length can be inferred by the scaling of the ratio $|t_L/V_L|$ with L . We first assume that $|A| < |B|$ (localized phase). Taking the large L limit we obtain

$$|t_L/V_L| = e^{-L/\xi_{\text{LE}}}, \text{ with } \xi_{\text{LE}} = 1/\log \left[\frac{|\frac{B}{\eta}| + \sqrt{(\frac{B}{\eta})^2 - 1}}{|\frac{A}{\eta}| + \sqrt{(\frac{A}{\eta})^2 - 1}} \right] , \quad (\text{S40})$$

where ξ_{LE} is the localization length. We can also compute the correlation length in the extended phase for $|A| > |B|$. This can be done just by interchanging A and B in the expression above, that is:

$$|V_L/t_L| = e^{-L/\xi_{\text{EL}}}, \text{ with } \xi_{\text{EL}} = 1/\log \left[\frac{|\frac{A}{\eta}| + \sqrt{(\frac{A}{\eta})^2 - 1}}{|\frac{B}{\eta}| + \sqrt{(\frac{B}{\eta})^2 - 1}} \right] , \quad (\text{S41})$$

where ξ_{EL} is the correlation length.

With all the ratios computed, we can summarize the different phases as in the main text, with the phase diagram being entirely analytically determined and only depending on $t_1 \equiv A(V, \eta, q)$, $V_1 \equiv B(V, \eta, p)$, $C_1 \equiv \eta$.

We will finish this section by cross-checking our correlation length results for the Aubry-André model. To get exactly the Hamiltonian in the original paper [1], we need to make $t \rightarrow te^p$ and $V \rightarrow Ve^q/2$ and then take the large p limit, with $p = q$. After doing so, we obtain

$$\begin{aligned} \frac{A}{\eta} &= -\cosh p + \frac{Ve^p}{2\eta} \sinh p \approx \frac{Ve^{2p}}{4\eta} \\ \frac{B}{\eta} &= -\cosh p + \frac{te^p}{\eta} \sinh p \approx \frac{te^{2p}}{2\eta}. \end{aligned} \quad (\text{S42})$$

This implies that

$$\begin{aligned} \xi_{\text{LE}} &= \frac{1}{\log \left(\frac{V}{2t} \right)}, \\ \xi_{\text{EL}} &= \frac{1}{\log \left(\frac{2t}{V} \right)} \end{aligned} \quad (\text{S43})$$

which are exactly the correlation lengths previously derived in [1].